# Microstrip Lines on Substrates with Segmented or Continuous Permittivity Profiles

Jean-Fu Kiang, *Member, IEEE*

***Abstract*— The propagation properties of microstrip lines on a substrate with inhomogeneous permittivity and conductivity profiles are analyzed. The eigenmodes in each inhomogeneous layer are obtained by solving an eigen equation. These eigenmodes are then used to formulate the Green's function of the stratified medium. An integral equation is next derived in terms of the surface current on the strip. Galerkin's method is then applied to obtain a determinantal equation to be solved for the propagation constant. The effect of several permittivity and conductivity profiles are analyzed.**

***Index Terms*— Dispersion relation, inhomogeneous substrate, microstrip line, stratified medium.**

## I. Introduction

FOR MICROSTRIP lines deposited on a segmented substrate, the expressions of potentials (quasi-TEM analyses) or fields (full-wave approaches) in the substrate become more complicated than the expressions in a homogeneous substrate. For a substrate with a continuous permittivity profile, explicit forms of eigenmodes are not available. Discretization approaches like finite difference method, finite element method, or method of lines can be resorted to obtain the potential or field distributions.

Using the quasi-TEM approximation, the proximity effect of a substrate edge on the capacitance of a microstrip line enclosed by a rectangular metal case has been studied [1], [2]. In [3], a spatial domain moment method is used to calculate the capacitance of two microstrip lines separated by a notch in the middle of the substrate. The notch serves to reduce the coupling between these two lines. In [4], a conformal mapping technique is derived to calculate the capacitance of a stripline embedded in a layered medium with rectangular-shape subdomains.

Using the full-wave approach, a method of lines has been developed to analyze the propagation properties of microstrip lines on a substrate of finite extent or on a substrate with notches [5]. A laterally open structure can be reduced to a closed one by using a coordinate transformation before the method of lines is applied to solve the propagation constant [6]. In [7], another method of lines is used to study the propagation properties of coplanar transmission lines on a semiconductor substrate. The permittivity profile of the substrate is a continuous function of a lateral coordinate.

In [8], microstrip lines on top of dielectric ridges are studied for their propagation and coupling characteristics. The Green's function is derived using the mode-matching technique, and an integral equation based on the current distribution on the strip surface is solved for the propagation constant. A similar approach with detailed derivation is given in [9] to solve a class of problems with striplines or slotlines embedded in a multilayered medium. The task to obtain the eigenmodes in each layer is laborious in [8] and [9].

In all these works except [7], the permittivity profile in each layer is assumed to be a piecewise constant function of the lateral coordinate. The continuous permittivity profile may occur when a microstrip line is deposited on a semiconductor substrate which contains doping zones with a different dielectric constant from that of the bulk substrate.

In this paper, a mode-matching technique is combined with the integral equation method to study the propagation properties of a single and two symmetrically coupled microstrip lines on a substrate. The permittivity profile of the substrate can be a piecewise continuous function of the lateral coordinate. First, the eigenmodes in each layer are obtained by solving a symmetric eigenvalue matrix equation. Reflection matrices are defined across the interfaces between two contiguous layers. Green's function is derived by inserting current dipoles in the layered medium. An integral equation is then formulated to express the tangential electric field in terms of the current on the strip surface. Galerkin's method is finally applied to solve the integral equation for the propagation constant.

## II. Formulation

In Fig. 1, we show the configuration of a microstrip line embedded in a layer ($l$) of a stratified medium. The whole structure is uniform in the $y$ direction. The dielectric constant in each layer is a piecewise continuous function of $x$ and is independent of $y$ and $z$. Two perfect electric conductor walls are put at $x = 0$ and $x = a$ to simplify the analysis.

First, we solve the eigenmodes in an inhomogeneous medium which extends to infinity in the $\pm z$ direction. The normal flux components $D_x$ and $B_x$ satisfy the following second-order ordinary differential equation:

$$\left[\nabla_s^2 + \epsilon(x)\frac{\partial}{\partial x}\epsilon^{-1}(x)\frac{\partial}{\partial x} + \omega^2\mu(x)\epsilon(x)\right]D_x(\bar{r}) = 0$$
$$\left[\nabla_s^2 + \mu(x)\frac{\partial}{\partial x}\mu^{-1}(x)\frac{\partial}{\partial x} + \omega^2\mu(x)\epsilon(x)\right]B_x(\bar{r}) = 0 \quad (1)$$

Manuscript received December 29, 1995; revised October 18, 1996. This work was supported by the National Science Council, Taiwan, R.O.C., under Contract NSC86-2221-E005-011.

The author is with the Department of Electrical Engineering, National Chung-Hsing University, Taichung, Taiwan, R.O.C.

Publisher Item Identifier S 0018-9480(97)00827-2.

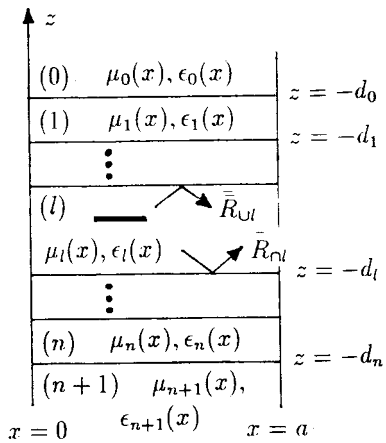


Fig. 1. Geometrical configuration of a microstrip line embedded in a stratified medium consisting of inhomogeneous layers.

where $\nabla_s^2 = \frac{\partial^2}{\partial y^2} + \frac{\partial^2}{\partial z^2}$. Assume that the waves propagate in the $y$ direction with a propagation constant $k_y$, $D_x$ can be expressed as

$$D_x(\bar{r}) = \sum_{n=1}^{\infty} a_n(z)\phi_n(x)e^{ik_y y} \tag{2}$$

where $\phi_n(x)$ is the eigensolution to

$$\left[\epsilon(x)\frac{d}{dx}\epsilon^{-1}(x)\frac{d}{dx} + \omega^2\mu(x)\epsilon(x)\right]\phi_n(x) = k_{ns}^2\phi_n(x) \tag{3}$$

and $k_{ns}^2$ is the corresponding eigenvalue. Choose one set of basis functions $S_p(x) = \sqrt{\varepsilon_p/a}\cos\alpha_p x$ with $\alpha_p = p\pi/a$ where $\varepsilon_p = 1$ when $p = 0$ and $\varepsilon_p = 2$ when $p \neq 0$. These basis functions satisfy the orthonormality specification that $\langle S_p(x), S_q(x)\rangle = \delta_{pq}$. The inner product is defined over the interval $0 \le x \le a$. The eigenmode $\phi_n(x)$ can be expressed in terms of $S_p(x)$ as

$$\phi_n(x) = \sum_{p=0}^{N-1} b_{np}S_p(x). \tag{4}$$

Substituting (4) into (3), and taking the inner product of $S_q(x)$ with the resulting equation

$$\sum_{p=0}^{N-1} M_{qp}b_{np} = k_{ns}^2 \sum_{p=0}^{N-1} N_{qp}b_{np}, \quad 0 \le q \le N-1 \tag{5}$$

where

$$\begin{aligned} M_{qp} =& -\langle S_q'(x), \epsilon^{-1}(x)S_p'(x)\rangle + \langle S_q(x), \omega^2\mu(x)S_p(x)\rangle \\ N_{qp} =& \langle S_q(x), \epsilon^{-1}(x)S_p(x)\rangle. \end{aligned} \tag{6}$$

The eigenvalues $k_{ns}^2$ and the corresponding eigenfunction $\phi_n(x)$ can be solved numerically from (5). Similarly, $B_x$ can be expressed as

$$B_x(\bar{r}) = \sum_{n=1}^{\infty} \tilde{a}_n(z)\tilde{\phi}_n(x)e^{ik_y y} \tag{7}$$

where $\tilde{\phi}_n(x)$ is the eigensolution to

$$\left[\mu(x)\frac{d}{dx}\mu^{-1}(x)\frac{d}{dx} + \omega^2\mu(x)\epsilon(x)\right]\tilde{\phi}_n(x) = \tilde{k}_{ns}^2\tilde{\phi}_n(x) \tag{8}$$

and $\tilde{k}_{ns}^2$ is the corresponding eigenvalue. Choose another set of basis functions $\tilde{S}_p(x) = \sqrt{2/a}\sin\alpha_p x$ with $\alpha_p = p\pi/a$. These basis functions satisfy the orthonormality specification that $\langle \tilde{S}_p(x), \tilde{S}_q(x)\rangle = \delta_{pq}$. The eigenmode $\tilde{\phi}_n(x)$ can be expressed in terms of $\tilde{S}_p(x)$ as

$$\tilde{\phi}_n(x) = \sum_{p=1}^{N} \tilde{b}_{np}\tilde{S}_p(x). \tag{9}$$

Substituting (9) into (8), and taking the inner product of $\tilde{S}_q(x)$ with the resulting equation, we have

$$\sum_{p=1}^{N} \tilde{M}_{qp}\tilde{b}_{np} = \tilde{k}_{ns}^2 \sum_{p=1}^{N} \tilde{N}_{qp}\tilde{b}_{np} \tag{10}$$

where

$$\begin{aligned} \tilde{M}_{qp} =& -\langle \tilde{S}_q'(x), \mu^{-1}(x)\tilde{S}_p'(x)\rangle + \langle \tilde{S}_q(x), \omega^2\epsilon(x)\tilde{S}_p(x)\rangle \\ \tilde{N}_{qp} =& \langle \tilde{S}_q(x), \mu^{-1}(x)\tilde{S}_p(x)\rangle. \end{aligned} \tag{11}$$

The eigenvalues $\tilde{k}_{ns}^2$ and the corresponding eigenfunction $\tilde{\phi}_n(x)$ can be solved numerically from (10). The eigenmodes $\phi_n(x)$ and $\tilde{\phi}_n(x)$ are normalized such that

$$\begin{aligned} \langle \phi_m(x), \epsilon^{-1}(x)\phi_n(x)\rangle &= \delta_{mn} \\ \langle \tilde{\phi}_m(x), \mu^{-1}(x)\tilde{\phi}_n(x)\rangle &= \delta_{mn}. \end{aligned} \tag{12}$$

The $E_y$ and $H_y$ components can be expressed in terms of $D_x$ and $B_x$ as [10]

$$\begin{aligned} E_y =& \sum_{n=1}^{\infty} \frac{1}{k_{sn}^2}\frac{ik_y}{\epsilon(x)}\frac{\partial}{\partial x}D_{nx} + \sum_{n=1}^{\infty} \frac{i\omega}{\tilde{k}_{sn}^2}\frac{\partial}{\partial z}B_{nx} \\ H_y =& \sum_{n=1}^{\infty} \frac{1}{\tilde{k}_{sn}^2}\frac{ik_y}{\mu(x)}\frac{\partial}{\partial x}B_{nx} - \sum_{n=1}^{\infty} \frac{i\omega}{k_{sn}^2}\frac{\partial}{\partial z}D_{nx} \end{aligned} \tag{13}$$

where $D_{nx}$ and $B_{nx}$ are the $n$th eigenmode components of $D_x$ and $B_x$, respectively.

Next, consider the fields generated by a line current $\bar{J}(\bar{r}) = \hat{y}I\delta(x - x_o)\delta(z - z_o)e^{ik_y y}$. From Maxwell's equations

$$\begin{aligned} &\left[\nabla_s^2 + \epsilon(x)\frac{\partial}{\partial x}\epsilon^{-1}(x)\frac{\partial}{\partial x} + \omega^2\mu(x)\epsilon(x)\right]D_x(\bar{r}) \\ &\qquad = I\frac{k_y}{\omega}e^{ik_y y}\delta'(x - x_o)\delta(z - z_o) \\ &\left[\nabla_s^2 + \mu(x)\frac{\partial}{\partial x}\mu^{-1}(x)\frac{\partial}{\partial x} + \omega^2\mu(x)\epsilon(x)\right]B_x(\bar{r}) \\ &\qquad = \mu I e^{ik_y y}\delta(x - x_o)\delta'(z - z_o). \end{aligned} \tag{14}$$

The solutions to (14) can be expressed in terms of the eigenmodes of (3) and (8) as

$$\bar{A}_x = \begin{bmatrix} D_x \\ B_x \end{bmatrix} = e^{ik_y y}\bar{\Phi}^t(x)\cdot e^{i\bar{\bar{K}}|z - z_o|}\cdot\bar{\psi}_\pm(x_o) \tag{15}$$

where

$$\bar{\Phi}^t(x) = \begin{bmatrix} \bar{\phi}^t(x) & 0 \\ 0 & \bar{\tilde{\phi}}^t(x) \end{bmatrix}$$
$$e^{i\bar{\bar{K}}|z-z_o|} = \begin{bmatrix} e^{i\bar{\bar{K}}_z|z-z_o|} & 0 \\ 0 & e^{i\bar{\bar{\tilde{K}}}_z|z-z_o|} \end{bmatrix}$$
$$\bar{\psi}_\pm(x_o) = \begin{bmatrix} \frac{ik_y}{2\omega\epsilon(x_o)} I\bar{\bar{K}}_z^{-1} \cdot \bar{\phi}'(x_o) \\ \pm\frac{I}{2}\bar{\tilde{\phi}}(x_o) \end{bmatrix} \quad (16)$$

$\bar{\phi}(x)$ is a column vector with $\bar{\phi}^t(x) = [\phi_1(x), \cdots, \phi_N(x)]$, $\bar{\tilde{\phi}}(x)$ is a column vector with $\bar{\tilde{\phi}}^t(x) = [\tilde{\phi}_1(x), \cdots, \tilde{\phi}_N(x)]$. $e^{i\bar{\bar{K}}_z|z-z_o|}$ is a diagonal matrix with the $\alpha$th diagonal component being $e^{ik_{\alpha z}|z-z_o|}$, $e^{i\bar{\bar{\tilde{K}}}_z|z-z_o|}$ is a diagonal matrix with the $\alpha$th diagonal component being $e^{i\tilde{k}_{\alpha z}|z-z_o|}$. $k_{\alpha z}$ and $\tilde{k}_{\alpha z}$ are related to the eigenvalues $k_{\alpha s}^2$ and $\tilde{k}_{\alpha s}^2$ by $k_{\alpha z}^2 = k_{\alpha s}^2 - k_y^2$, $\tilde{k}_{\alpha z}^2 = \tilde{k}_{\alpha s}^2 - k_y^2$. $\bar{\bar{K}}_z$ is a diagonal matrix $\text{diag.}[k_{1z}, \cdots, k_{Nz}]$. Substituting (15) into (13), we obtain

$$\bar{A}_y = \begin{bmatrix} H_y \\ E_y \end{bmatrix} = e^{ik_y y}\bar{\bar{N}}_\pm(x) \cdot e^{i\bar{\bar{K}}|z-z_o|} \cdot \bar{\psi}_\pm(x_o) \quad (17)$$

where

$$\bar{\bar{N}}_\pm(x) = \begin{bmatrix} \pm\omega\bar{\phi}^t(x) \cdot \bar{\bar{K}}_s^{-2} \cdot \bar{\bar{K}}_z & ik_y\mu^{-1}\bar{\tilde{\phi}}^{t'}(x) \cdot \bar{\bar{\tilde{K}}}_s^{-2} \\ ik_y\epsilon^{-1}\bar{\phi}^{t'}(x) \cdot \bar{\bar{\tilde{K}}}_s^{-2} & \mp\omega\bar{\tilde{\phi}}^t(x) \cdot \bar{\bar{\tilde{K}}}_s^{-2} \cdot \bar{\bar{\tilde{K}}}_z \end{bmatrix} \quad (18)$$

where $\bar{\bar{K}}_s^{-2}$ and $\bar{\bar{\tilde{K}}}_s^{-2}$ are diagonal matrices with $\bar{\bar{K}}_s^{-2} = \text{diag.}[k_{1s}^{-2}, \cdots, k_{Ns}^{-2}]$ and $\bar{\bar{\tilde{K}}}_s^{-2} = \text{diag.}[\tilde{k}_{1s}^{-2}, \cdots, \tilde{k}_{Ns}^{-2}]$.

Next, assume that a line current is located in layer ($l$) of a stratified medium, the fields in layer ($l$) can thus be expressed as

$$\bar{A}_{lx} = e^{ik_y y}\bar{\Phi}_l^t(x) \cdot \left[e^{i\bar{\bar{K}}_l|z_l-z_l'|} \cdot \bar{\psi}_\pm(x_o) + e^{i\bar{\bar{K}}_l z_l} \cdot \bar{\alpha}_l + e^{-i\bar{\bar{K}}_l z_l} \cdot \bar{\beta}_l\right] \quad (19)$$

where $z_l = z + d_l$, $z_l' = z_o + d_l$, the subscript $l$ indicates that the expression is for layer ($l$). Define a reflection matrix $\bar{\bar{R}}_{\cap l}$ at the interface $z = -d_l$ such that the reflection matrix multiplied by the downward-going component gives the upward-going components, i.e.,

$$\bar{\bar{R}}_{\cap l} \cdot \left[e^{i\bar{\bar{K}}_l z_l'} \cdot \bar{\psi}_-(x_o) + \bar{\beta}_l\right] = \bar{\alpha}_l. \quad (20)$$

Similarly, define another reflection matrix $\bar{\bar{R}}_{\cup l}$ at $z = -d_{l-1}$ such that

$$\bar{\bar{R}}_{\cup l} \cdot \left[e^{i\bar{\bar{K}}_l(h_l - z_l')} \cdot \bar{\psi}_+(x_o) + e^{i\bar{\bar{K}}_l h_l} \cdot \bar{\alpha}_l\right] = e^{-i\bar{\bar{K}}_l h_l} \cdot \bar{\beta}_l. \quad (21)$$

Then, $\bar{\alpha}_l$ and $\bar{\beta}_l$ can be solved from (20) and (21) to be

$$\begin{aligned} \bar{\alpha}_l =& \left[\bar{\bar{I}} - \bar{\bar{R}}_{\cap l} \cdot e^{i\bar{\bar{K}}_l h_l} \cdot \bar{\bar{R}}_{\cup l} \cdot e^{i\bar{\bar{K}}_l h_l}\right]^{-1} \\ &\cdot [\bar{\bar{R}}_{\cap l} \cdot e^{i\bar{\bar{K}}_l z_l'} \cdot \bar{\psi}_-(x_o) + \bar{\bar{R}}_{\cap l} \\ &\cdot e^{i\bar{\bar{K}}_l h_l} \cdot \bar{\bar{R}}_{\cup l} \cdot e^{i\bar{\bar{K}}_l(h_l - z_l')} \cdot \bar{\psi}_+(x_o)] \\ \bar{\beta}_l =& \left[\bar{\bar{I}} - e^{i\bar{\bar{K}}_l h_l} \cdot \bar{\bar{R}}_{\cup l} \cdot e^{i\bar{\bar{K}}_l h_l} \cdot \bar{\bar{R}}_{\cap l}\right]^{-1} \\ &\cdot \left[e^{i\bar{\bar{K}}_l h_l} \cdot \bar{\bar{R}}_{\cup l} \cdot e^{i\bar{\bar{K}}_l(h_l - z_l')} \cdot \bar{\psi}_+(x_o) + e^{i\bar{\bar{K}}_l h_l}\right. \\ &\left.\cdot \bar{\bar{R}}_{\cup l} \cdot e^{i\bar{\bar{K}}_l h_l} \cdot \bar{\bar{R}}_{\cap l} \cdot e^{i\bar{\bar{K}}_l z_l'} \cdot \bar{\psi}_-(x_o)\right]. \end{aligned} \quad (22)$$

Using the reflection matrices, the fields in layer ($m$) with $m > l$ can be expressed as

$$\begin{aligned} \bar{A}_{mx} &= e^{ik_y y}\bar{\Phi}_m^t(x) \cdot \left[e^{i\bar{\bar{K}}_m z_m} \cdot \bar{\bar{R}}_{\cap m} + e^{-i\bar{\bar{K}}_m z_m}\right] \cdot \bar{\beta}_m \\ \bar{A}_{my} &= e^{ik_y y}[\bar{\bar{N}}_{m+}(x) \cdot e^{i\bar{\bar{K}}_m z_m} \cdot \bar{\bar{R}}_{\cap m} \\ &\quad + \bar{\bar{N}}_{m-}(x) \cdot e^{-i\bar{\bar{K}}_m z_m}] \cdot \bar{\beta}_m. \end{aligned} \quad (23)$$

By imposing the boundary condition that $\bar{A}_{rx} = \bar{A}_{(r+1)x}$ and $\bar{A}_{ry} = \bar{A}_{(r+1)y}$ at $z = -d_r$, we obtain the recursive relation between the reflection matrices as

$$\begin{aligned} \bar{\bar{R}}_{\cap r} =& \left\{\left[\bar{\bar{I}} + e^{i\bar{\bar{K}}_{r+1}h_{r+1}} \cdot \bar{\bar{R}}_{\cap(r+1)} \cdot e^{i\bar{\bar{K}}_{r+1}h_{r+1}}\right]^{-1} \cdot \bar{\bar{B}}_{r(r+1)}^t\right. \\ &- \left[\bar{\bar{H}}_{r(r+1)+} \cdot e^{i\bar{\bar{K}}_{r+1}h_{r+1}} \cdot \bar{\bar{R}}_{\cap(r+1)} \cdot e^{i\bar{\bar{K}}_{r+1}h_{r+1}}\right. \\ &\left.\left.+\bar{\bar{H}}_{r(r+1)-}\right]^{-1} \cdot \bar{\bar{H}}_{rr+}\right\}^{-1} \\ &\cdot \left\{\left[\bar{\bar{H}}_{r(r+1)+} \cdot e^{i\bar{\bar{K}}_{r+1}h_{r+1}} \cdot \bar{\bar{R}}_{\cap(r+1)} \cdot e^{i\bar{\bar{K}}_{r+1}h_{r+1}}\right.\right. \\ &\left.+\bar{\bar{H}}_{r(r+1)-}\right]^{-1} \cdot \bar{\bar{H}}_{rr-} \\ &\left.- \left[\bar{\bar{I}} + e^{i\bar{\bar{K}}_{r+1}h_{r+1}} \cdot \bar{\bar{R}}_{\cap(r+1)} \cdot e^{i\bar{\bar{K}}_{r+1}h_{r+1}}\right]^{-1} \cdot \bar{\bar{B}}_{r(r+1)}^t\right\} \end{aligned} \quad (24)$$

where

$$\begin{aligned} \bar{\bar{B}}_{pq} &= \int_0^a dx \bar{\Phi}_p(x) \cdot \begin{bmatrix} \epsilon_p^{-1}(x) & 0 \\ 0 & \mu_p^{-1}(x) \end{bmatrix} \cdot \bar{\Phi}_q^t(x) \\ \bar{\bar{H}}_{pq\pm} &= \int_0^a dx \bar{\Phi}_p(x) \cdot \bar{\bar{N}}_{q\pm}(x). \end{aligned} \quad (25)$$

Similarly, the fields in layer ($m$) with $m < l$ can be expressed as

$$\begin{aligned} \bar{A}_{mx} &= e^{ik_y y}\bar{\Phi}_m^t(x) \cdot [e^{i\bar{\bar{K}}_m z_m} \\ &\quad + e^{i\bar{\bar{K}}_m(h_m - z_m)} \cdot \bar{\bar{R}}_{\cup m} \cdot e^{i\bar{\bar{K}}_m h_m}] \cdot \bar{\alpha}_m \\ \bar{A}_{my} &= e^{ik_y y}[\bar{\bar{N}}_{m+}(x) \cdot e^{i\bar{\bar{K}}_m z_m} \\ &\quad + \bar{\bar{N}}_{m-}(x) \cdot e^{i\bar{\bar{K}}_m(h_m - z_m)} \cdot \bar{\bar{R}}_{\cup m} \cdot e^{i\bar{\bar{K}}_m h_m}] \cdot \bar{\alpha}_m. \end{aligned} \quad (26)$$

By imposing the boundary condition that $\bar{A}_{rx} = \bar{A}_{(r+1)x}$ and $\bar{A}_{ry} = \bar{A}_{(r+1)y}$ at $z = -d_r$, we obtain the recursive relation between the reflection matrices as

$$\begin{aligned}\bar{\bar{R}}_{\cup(r+1)} =&\Big\{\Big[\bar{\bar{I}} + e^{i\bar{\bar{K}}_r h_r}\cdot\bar{\bar{R}}_{\cup r}\cdot e^{i\bar{\bar{K}}_r h_r}\Big]^{-1}\cdot\Big(\bar{\bar{B}}^t_{r(r+1)}\Big)^{-1}\\ &-\Big[\bar{\bar{H}}_{rr+} + \bar{\bar{H}}_{rr-}\cdot e^{i\bar{\bar{K}}_r h_r}\cdot\bar{\bar{R}}_{\cup r}\cdot e^{i\bar{\bar{K}}_r h_r}\Big]^{-1}\\ &\cdot\bar{\bar{H}}_{r(r+1)-}\Big\}^{-1}\\ &\cdot\Big\{\Big[\bar{\bar{H}}_{rr+} + \bar{\bar{H}}_{rr-}\cdot e^{i\bar{\bar{K}}_r h_r}\cdot\bar{\bar{R}}_{\cup r}\cdot e^{i\bar{\bar{K}}_r h_r}\Big]^{-1}\\ &\cdot\bar{\bar{H}}_{r(r+1)+} - \Big[\bar{\bar{I}} + e^{i\bar{\bar{K}}_r h_r}\cdot\bar{\bar{R}}_{\cup r}\cdot e^{i\bar{\bar{K}}_r h_r}\Big]^{-1}\\ &\cdot\Big(\bar{\bar{B}}^t_{r(r+1)}\Big)^{-1}\Big\}. \qquad (27)\end{aligned}$$

Next, consider the fields generated by another line current $\bar{J}(\bar{r}) = \hat{x}I\delta(x-x_o)\delta(z-z_o)e^{ik_y y}$. From Maxwell's equations $B_x = 0$ and $D_x$ satisfy

$$\begin{aligned}&\left[\nabla_s^2 + \epsilon(x)\frac{\partial}{\partial x}\epsilon^{-1}(x)\frac{\partial}{\partial x} + \omega^2\mu(x)\epsilon(x)\right]D_x(\bar{r})\\ &\quad = -i\omega\mu\epsilon I e^{ik_y y}\delta(x-x_o)\delta(z-z_o)\\ &\quad + \epsilon\frac{\partial}{\partial x}\epsilon^{-1}\frac{I}{i\omega}e^{ik_y y}\delta'(x-x_o)\delta(z-z_o). \qquad (28)\end{aligned}$$

The solution to (28) is

$$\bar{A}_x = \begin{bmatrix} D_x \\ B_x \end{bmatrix} = e^{ik_y y}\bar{\Phi}^t(x)\cdot e^{i\bar{\bar{K}}|z-z_o|}\cdot\bar{\xi}_\pm(x_o) \qquad (29)$$

where

$$\bar{\xi}_\pm(x_o) = \begin{bmatrix} -I\frac{\omega\mu(x_o)}{2}\bar{\bar{K}}_z^{-1}\cdot\bar{\phi}(x_o) - I\frac{1}{2\omega\epsilon(x_o)}\bar{\bar{K}}_z^{-1}\cdot\bar{\phi}''(x_o) \\ 0 \end{bmatrix}. \qquad (30)$$

Substituting (29) into (13), we obtain

$$\bar{A}_y = \begin{bmatrix} H_y \\ E_y \end{bmatrix} = e^{ik_y y}\bar{\bar{N}}^t_\pm(x)\cdot e^{i\bar{\bar{K}}|z-z_o|}\cdot\bar{\xi}_\pm(x_o). \qquad (31)$$

When the line current source is located in layer ($l$) of a stratified medium, the field expressions are the same as (19) except that $\bar{\psi}$ is replaced by $\bar{\xi}$.

A microstrip line located in layer ($l$) can be perceived as a superposition of line current source on the strip $c \le x \le d$ as

$$\begin{aligned}\bar{J}(x,y) =& [\hat{x}J_x(x) + \hat{y}J_y(x)]e^{ik_y y}\delta(z-z_o),\\ & c \le x \le d. \qquad (32)\end{aligned}$$

Thus, the tangential field components in layer ($l$) can be expressed as

$$\begin{aligned}\bar{A}_{lx} =& \int_c^d dx' J_x(x')e^{ik_y y}\bar{\Phi}^t_l(x)\\ &\cdot\Big[e^{i\bar{\bar{K}}_l|z_l-z'_l|}\cdot\bar{\xi}_\pm(x') + e^{i\bar{\bar{K}}_l z_l}\cdot\bar{\alpha}'_l + e^{-i\bar{\bar{K}}_l z_l}\cdot\bar{\beta}'_l\Big]\\ &+\int_c^d dx' J_y(x')e^{ik_y y}\bar{\Phi}^t_l(x)\\ &\cdot\Big[e^{i\bar{\bar{K}}_l|z_l-z'_l|}\cdot\bar{\psi}_\pm(x') + e^{i\bar{\bar{K}}_l z_l}\cdot\bar{\alpha}_l + e^{-i\bar{\bar{K}}_l z_l}\cdot\bar{\beta}_l\Big]\\ \bar{A}_{ly} =& \int_c^d dx' J_x(x')e^{ik_y y}\\ &\cdot\Big[\bar{\bar{N}}_{l\pm}(x)\cdot e^{i\bar{\bar{K}}_l|z_l-z'_l|}\cdot\bar{\xi}_\pm(x') + \bar{\bar{N}}_{l+}(x)\cdot e^{i\bar{\bar{K}}_l z_l}\cdot\bar{\alpha}'_l\\ &+\bar{\bar{N}}_{l-}(x)\cdot e^{-i\bar{\bar{K}}_l z_l}\cdot\bar{\beta}'_l\Big]\\ &+\int_c^d dx' J_y(x')e^{ik_y y}\\ &\cdot\Big[\bar{\bar{N}}_{l\pm}(x)\cdot e^{i\bar{\bar{K}}_l|z_l-z'_l|}\cdot\bar{\psi}_\pm(x')\\ &+\bar{\bar{N}}_{l+}(x)\cdot e^{i\bar{\bar{K}}_l z_l}\cdot\bar{\alpha}_l + \bar{\bar{N}}_{l-}(x)\cdot e^{-i\bar{\bar{K}}_l z_l}\cdot\bar{\beta}_l\Big] \qquad (33)\end{aligned}$$

where $\bar{\alpha}_l$ and $\bar{\beta}_l$ are given in (22), and $\bar{\alpha}'_l$ and $\bar{\beta}'_l$ have the same forms except that $\bar{\psi}_\pm$ is replaced by $\bar{\xi}_\pm$.

Next, impose the boundary conditions that the tangential electric field vanishes on the strip surface to obtain an integral equation with the surface current as the unknown variable. To apply the Galerkin's method, we first choose a set of basis functions to represent $J_x(x)$ and $J_y(x)$ on the strip surface. Substitute the current distribution in terms of these basis functions into the integral equation, then take the inner product of another set of weighting functions with the resulting equation to form a determinantal equation. The dispersion relation is obtained by solving the determinantal equation.

## III. Numerical Results

In Fig. 2, we show the phase constant of a microstrip line on a segmented substrate. The results with a homogeneous substrate [11] match reasonably well with our results in the high-frequency range. The deviation in the low-frequency range is because we model a laterally closed structure while the structure in [11] is laterally open.

In Fig. 3, we show the phase constant of a microstrip line on a substrate with a parabolic permittivity profile. The maximum or minimum dielectric constant $\epsilon_m$, occurs at the middle of the substrate. The curve with $\epsilon_m = 10$ is that of a homogeneous substrate.

In Fig. 4, we show the phase constant of a microstrip line on a substrate with a homogeneous dielectric constant and a parabolic conductivity profile. The maximum or minimum conductivity $\sigma_m$ occurs at the middle of the substrate. The phase constant at the low-frequency range increases as the conductivity increases. The slow-wave phenomenon is obvious for $\sigma = 10$ ℧/m. The associated attenuation constant in

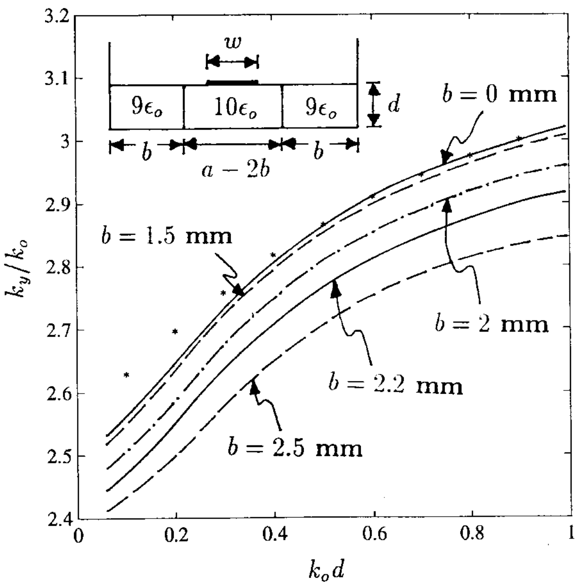


Fig. 2. Normalized phase constant of a microstrip line on a segmented substrate, $a = 5$ mm, $d = 1$ mm, $w = 1$ mm, * : results with a homogeneous layer ($b = 0$) in [11].

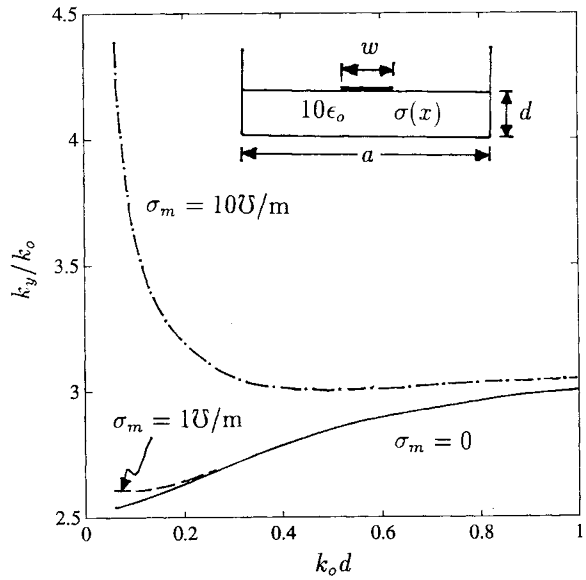


Fig. 4. Normalized phase constant of a microstrip line on a substrate with a parabolic conductivity profile $\sigma(x) = 4\sigma_m x(a - x)/a^2$, $a = 5$ mm, $d = 1$ mm, $w = 1$ mm.

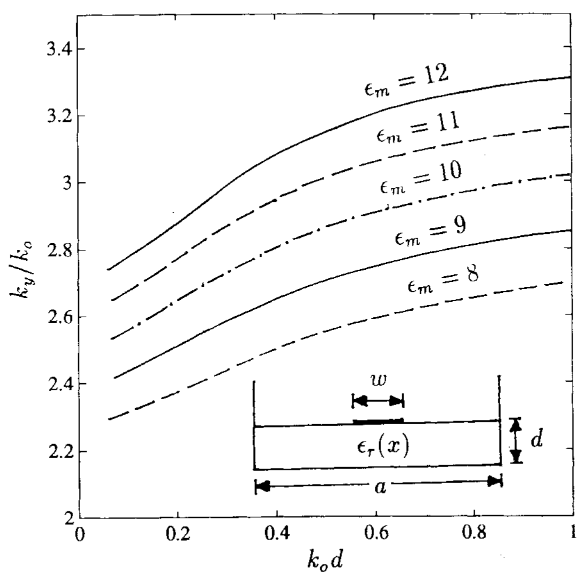


Fig. 3. Normalized phase constant of a microstrip line on a substrate with a parabolic permittivity profile $\epsilon_r(x)/\epsilon_o = 10 + 4(\epsilon_m - 10)x(a - x)/a^2$, $a = 5$ mm, $d = 1$ mm, $w = 1$ mm.

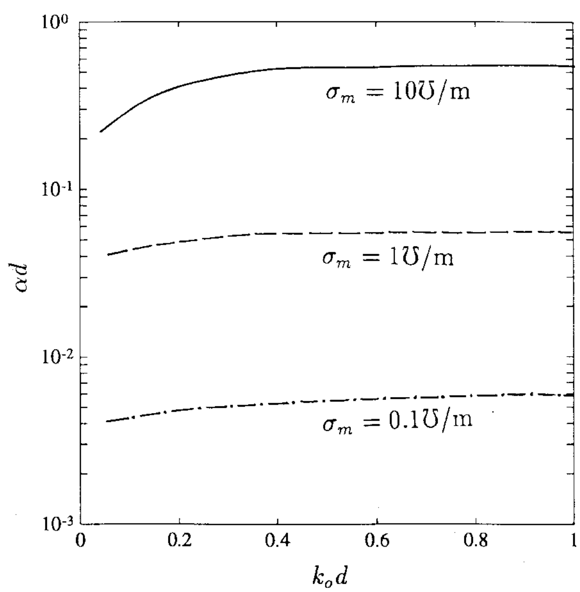


Fig. 5. Attenuation constant of a microstrip line on a substrate with a parabolic conductivity profile, all the parameters are the same as in Fig. 4.

Fig. 5 indicates that the loss is roughly proportional to the conductivity at least in the range of $0.1 < \sigma_m < 10$ ℧/m and decreases at low frequencies.

In Fig. 6, we show the phase constant of the even mode of two symmetrically coupled microstrip lines on a substrate with a parabolic permittivity profile. The results with a homogeneous substrate [11] are also shown for comparison. The deviation between our results and those in [11] at low frequencies can be explained in the same way as for the single microstrip line. The phase constant for the corresponding odd mode is shown in Fig. 7. Our results and those in [11] match well in the low-frequency range because the field distribution of the odd mode tends to concentrate between the two strips, hence the side walls have less effect on the odd mode than on the even mode.

The phase constant and the attenuation constant for two symmetrically coupled microstrip lines on a substrate with a homogeneous permittivity and a parabolic conductivity profile are shown in Figs. 8 and 9. The slow-wave phenomenon is observed for both the even and the odd modes at low frequencies, especially with higher conductivity. The attenuation constant of the even mode is higher than that of the odd mode because the electric field of the odd mode tends to concentrate between the two strips, while that of the even mode spreads to

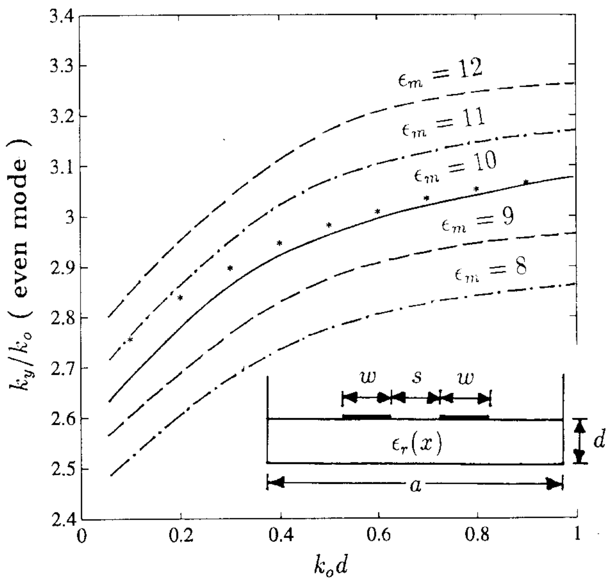


Fig. 6. Normalized phase constant of the even mode of two symmetrically coupled microstrip lines on a substrate with a parabolic permittivity profile $\epsilon_r(x)/\epsilon_o = 10 + 4(\epsilon_m - 10)x(a-x)/a^2$, $a = 6.4$ mm, $d = 1$ mm, $w = 1$ mm, $s = 0.4$ mm, * : results with a homogeneous layer ($\epsilon_m = 10$) in [11].

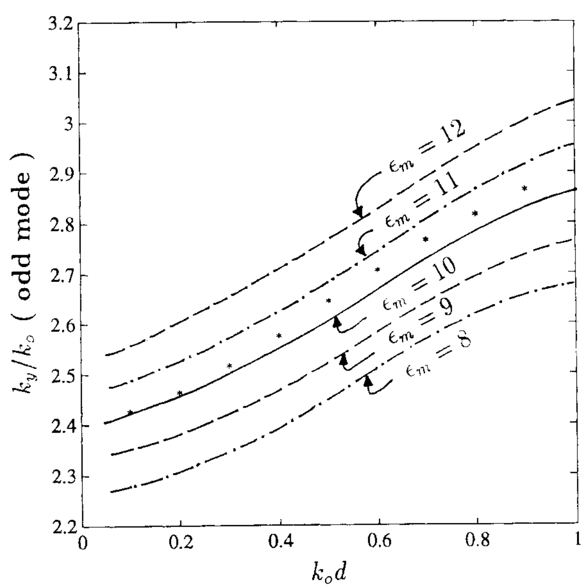


Fig. 7. Normalized phase constant of the odd mode of two symmetrically coupled microstrip lines on a substrate with a parabolic permittivity profile; all the parameters are the same as in Fig. 6.

a larger extent in the substrate. Hence, the electric field of the even mode incurs more attenuation than that of the odd mode.

## IV. Conclusion

We have applied a mode-matching technique and the integral equation method to study the propagation properties of a single and two symmetrically coupled microstrip lines embedded in a stratified medium where the permittivity and conductivity profiles in each layer can be continuous functions of the lateral coordinate. The phase constant and the attenuation constant with various inhomogeneous profiles have been obtained by this method. Slow-wave phenomenon is also observed for structures with a lossy substrate.

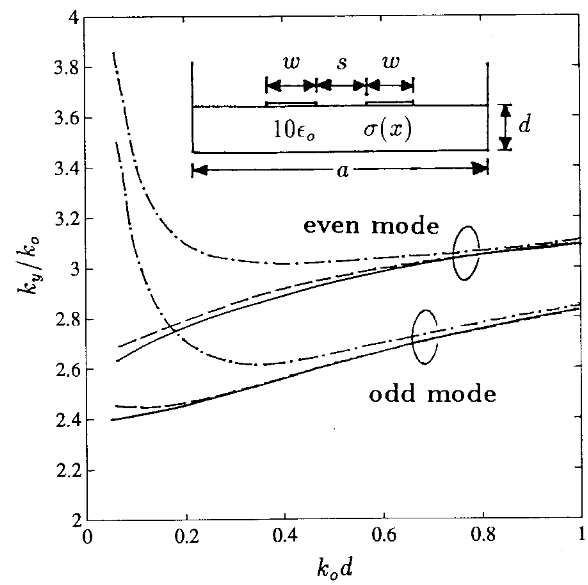


Fig. 8. Normalized phase constant of two symmetrically coupled microstrip lines on a substrate with a parabolic conductivity profile $\sigma(x) = 4\sigma_m x(a-x)/a^2$, $a = 6.4$ mm, $d = 1$ mm, $w = 1$ mm, $s = 0.4$ mm. (_____): $\sigma = 0.1$ ℧/m, (- - - -): $\sigma = 1$ ℧/m, (- - - -): $\sigma = 10$ ℧/m.

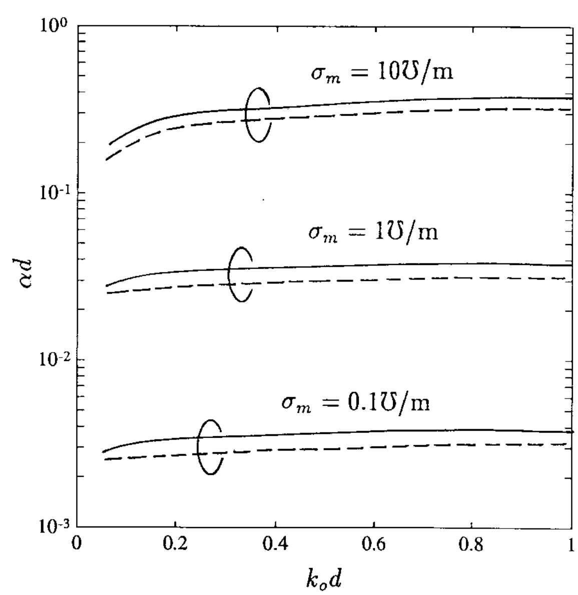


Fig. 9. Attenuation constant of two symmetrically coupled microstrip lines on a substrate with a parabolic conductivity profile, all the parameters are the same as in Fig. 8. (_____): even mode, (- - - -): odd mode.

## Acknowledgment

The author would like to thank the reviewers for their useful comments in revising this paper.

## References

[1] E. Yamashita, H. Ohashi, and K. Atsuki, ''Characterization of microstrip lines near a substrate edge and design formulas of edge-compensated microstrip lines,'' *IEEE Trans. Microwave Theory Tech.*, vol. 37, pp. 890–896, May 1989.

[2] K. Li and Y. Fujii, ''Indirect boundary element method applied to generalized microstripline analysis with applications to side-proximity effect in MMIC's,'' *IEEE Trans. Microwave Theory Tech.*, vol. 40, pp. 237–244, Feb. 1992.

[3] S. He, A. Z. Elsherbeni, and C. E. Smith, ‘‘Decoupling between two conductor microstrip transmission lines,’’ *IEEE Trans. Microwave Theory Tech.*, vol. 41, pp. 53–61, Jan. 1993.

[4] A. Nyshadham and K. V. S. Rao, ‘‘Analysis of stripline filled with multiple dielectric regions,’’ *IEEE Trans. Microwave Theory Tech.*, vol. 39, pp. 151–155, Jan. 1991.

[5] M. Thorburn, A. Agoston, and V. K. Tripathi, ‘‘Computation of frequency-dependent propagation characteristics of microstriplike propagation structures with discontinuous layers,’’ *IEEE Trans. Microwave Theory Tech.*, vol. 38, pp. 148–153, Feb. 1990.

[6] X. H. Yang and L. Shafai, ‘‘Full-wave approach for the analysis of open planar waveguides with finite width dielectric layers and ground planes,’’ *IEEE Trans. Microwave Theory Tech.*, vol. 42, pp. 142–149, Jan. 1994.

[7] K. Wu and R. Vahldieck, ‘‘Hybrid-mode analysis of homogeneously and inhomogeneously doped low-loss slow-wave coplanar transmission lines,’’ *IEEE Trans. Microwave Theory Tech.*, vol. 39, pp. 1348–1360, Aug. 1991.

[8] A. G. Engel, Jr., and L. P. B. Katehi, ‘‘Frequency and time domain characterization of microstrip-ridge structures,’’ *IEEE Trans. Microwave Theory Tech.*, vol. 41, pp. 1251–1262, Aug. 1993.

[9] J.-W. Huang and C.-K. C. Tzuang, ‘‘Green’s impedance function approach for propagation characteristics of generalized striplines and slotlines on nonlayered substrates,’’ *IEEE Trans. Microwave Theory Tech.*, vol. 42, pp. 2317–2327, Dec. 1994.

[10] W. C. Chew, ‘‘Modeling of the dielectric logging tool at high frequencies: theory,’’ *IEEE Trans. Geosci. Remote Sensing*, vol. 26, pp. 382–387, July 1988.

[11] J. B. Knorr and A. Tufekcioglu, ‘‘Spectral-domain calculation of microstrip characteristic impedance,’’ *IEEE Trans. Microwave Theory Tech.*, vol. MTT–23, pp. 725–728, Sept. 1975.

**Jean-Fu Kiang** (M’89) was born in Taipei, Taiwan, R.O.C., on February 2, 1957. He received the B.S.E.E. and MSEE degrees from National Taiwan University, Taiwan, R.O.C., and the Ph.D. degree from Massachusetts Institute of Technology, Cambridge, MA, in 1979, 1981, and 1989, respectively.

He has been with IBM Watson Research Center, Bellcore, and Siemens. He is currently with the Department of Electrical Engineering, National Chung-Hsing University, Taichung, Taiwan, R.O.C.